ARCHIVE OF MECHANICAL ENGINEERING

DOI: 10.24425/ame.2023.145583 2023, Vol. 70, No. 2, pp. 247–270

Pallavi KHAIRE [1,2], Vikas PHALLE[1]

A smart fault identification system for ball bearing using simulation-driven vibration analysis

Received 14 November 2022, **Revised** 18 April 2023, **Accepted** 28 April 2023, **Published online** 19 June 2023

Keywords: condition monitoring, bearing defect, FFT analyzer, BPFI, BPFO, multiclass support vector machine

Bearings are one of the pivotal parts of rotating machines. The health of a bearing is responsible for the hassle-free operation of a machine. As vibration signatures give intimations of machine failure at an earlier stage, mostly vibration-based condition monitoring is used to monitor bearing's health for avoiding the risk of failure. In this work, a simulation-based approach is adopted to identify surface defects at ball bearing raceways. The vibration data in time and frequency domain is captured by FFT analyzer from an experimental setup. The time frequency domain conversion of a raw time domain data was carried out by wavelet packet transform, as it takes into account the transients and spectral frequencies. The rotor bearing model is simulated in ANSYS. Finally, most influencing statistical features were extracted by employing Principal Component Analysis, and fed to Multiclass Support Vector Machine. To train the algorithm, the simulated data is used whereas the data acquired from FFT analyzer is used for testing. It can be concluded that the defects are characterized by Ball Pass Frequency at inner race and outer raceway as indicated in the literature. The developed model is capable to monitor bearing's health which gives an average accuracy of 99%.

1. Introduction

Most of rotating machines have rolling element bearings as an integrated part of it. Machine's functionality may lead to a failure if the bearing faults remain undetected. Thus, it is very essential to monitor bearing's health for uninterrupted machine operation. For checking the bearing's health, a brief study related to

✉ Pallavi KHAIRE, e-mail: Pallavi.khaire@fcrit.ac.in

[1]Veermata Jijabai Technological Institute, Mumbai, India. ORCID: 0000-0001-8485-7439

[2]Fr. C. Rodrigues Institute of Technology, Navi Mumbai, India

bearing defects has to be carried out. Also, the causes of bearing defects have to be analyzed and corrective measures should be taken to prevent the machine's downtime and related monetary losses.

The foremost thing in condition monitoring is to understand how severely the bearing faults affect the functionality of the machine and their vibration characteristics. It is very essential to identify the bearing defects at the earliest to avoid other components failure and ultimately machine failure. The usual defects in a ball bearing are observed as a defect at inner raceway, defect at outer raceway and defect in ball. There is a possibility that one fault may be responsible for the occurrence of another and this fact cannot be ignored. The goal of the proposed work is to discover faults occurring at inner and outer race of a ball bearing by developing a simulation-driven machine learning model. An extensive literature review was been performed related to vibration-based condition monitoring techniques with a machine learning approach.

Taha et al. [1] presented two methodologies to identify bearing faults by acquiring their vibration responses. The first methodology deals with running the bearing till its failure. This approach is laborious and tedious as it takes a lot of time and one has to wait for bearing to fail. Therefore, in another methodology, the authors purposely created defects in bearing and observed the vibration spectrums of bearings having faults. They concluded that the high amplitude at Ball Pass Frequency at Outer Race (BPFO) and Ball pass Frequency at Inner Race (BPFI) are the signs of the existence of outer and inner race defects respectively. Pratesh et al. [2] have identified bearing faults using data-driven machine learning approach. The experimental test rig for simulating faults was developed. Three faults were considered for the study, viz. defect at inner race, outer race and defect in ball. The preprocessing of raw data was carried out using the wavelet transform. Two machine learning algorithms, Artificial Neural Networks (ANN) and Fuzzy Rules were used to identify the defects. The suggested methodologies are good in predicting bearing defects. Rao [3] did a comparative analysis between the methodology using vibration signatures and the methodology using acoustic waves to identify faults in a cylindrical roller bearing and their severity. From the results, it was observed that the acoustic waves methodology is definitively more effective than vibration analysis. Shah and Guha [4] proposed a method based on extracting a statistical feature, kurtosis from the time domain vibration spectrum of a defective bearing. They have used Empirical Mode Decomposition (EMD) to pull out inherent mode functions and remove noise. The methodology is quite reliable for detecting faulty bearings. Ratnam et al. [5] used a data-driven approach using acoustic emission instead of vibration analysis. They have also used machine learning techniques, such as ANN and SVM, to detect fault present at outer race and its severity. The defect intensity can be identified by using machine learning model and it was noticed that ANN gives a better size prediction as compared to SVM with an error of 6.57%.

Karthik and Nataraj [6] followed a theoretical approach to identify the fault at the outer race of a ball bearing. When a signal wave passes through a defect, the modulation can be observed. The approach followed this principle and it was concluded that the modulation shape is a function of the width of the defect. The maximum amplitude is seen at BPFO and its harmonics along with side bands for faulty bearing whereas for healthy bearing it appears at 1X of the operating frequency. Kankar et al. [7] presented a ball-bearing fault identification model using machine learning. They have used Artificial Neural Networks (ANN) and Support Vector Machines (SVM) for fault prediction. They concluded that by introducing machine learning along with vibration analysis, bearing defects can be detected automatically. Sharma A. et al. [8] concluded that a comparative study between ANN and CNN shows that machine learning is an efficient and effective method for detecting defects and their severity.

It can be unveiled from the literature review that it is particularly essential to identify bearing defects at the earliest for enhancing the machine's life. Very few researchers have considered the combination of bearing faults with varying severity. As far as the author's knowledge is concerned based on the research work available in the literature, the work comprising a machine learning approach using experimental, simulation data for the combination of faults with different severity levels of fault at different operating speeds is not available. To fill this gap in the literature, the proposed machine learning model is developed to identify the combination of faults in bearings with different levels of severity of defect at different operating speeds.

2. Laboratory test setup for bearing fault Identification

A bearing fault diagnosis arrangement used to collect vibration data for healthy and defective bearings, which can be seen in Fig. 1 and Fig. 2, shows the schematic representation of the experimental arrangement. The spectra quest experimental

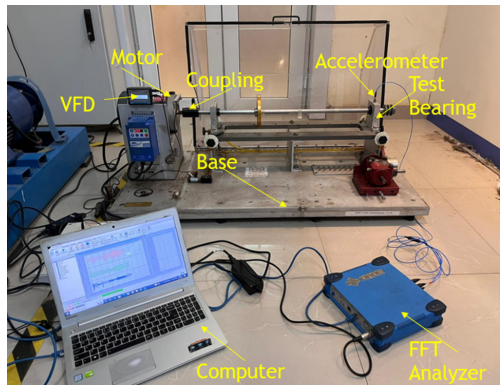

Fig. 1. The experimental setup

arrangement is comprised of 1 HP D.C. motor having an operating range up to 6000 rpm. Two deep groove ball bearings (SKF 6305) with housing are used in the experimental setup. First, a bearing (8) is used to support the driving end of the shaft, and the driven shaft is held by using two bearings, (9) and (8). The motor and the driven shaft are connected by using a flexible type coupling (3).

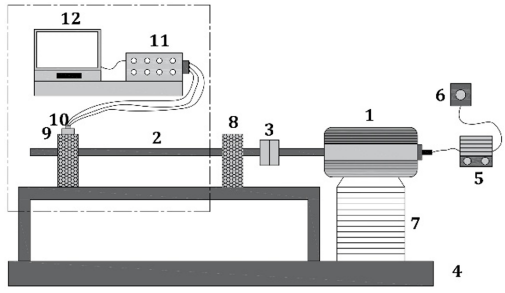

Fig. 2. Schematic representation of the experimental fault diagnosis setup: 1 – motor, 2 – shaft, 3 – flexible coupling, 4 – base, 5 – VFD, 6 – power supply, 7 – motor base, 8 – driven shaft bearing, 9 – test bearing, 10 – triaxial accelerometer, 11 – data acquisition system, 12 – computer

The end bearing supporting the driven shaft is used as the test bearing for acquiring vibration data. The faulty bearings were prepared by creating defects on inner and outer race with a varying severity of 0.25 mm to 0.5 mm. Wire cut EDM method was used to create rectangular notch at inner and outer race to resemble its behavior with crack. A notch of 0.5 mm on inner race that can be seen in Fig. 3 is considered as an inner race fault.

Fig. 3. 0.5 mm fault at inner race

To measure the vibration, a triaxial accelerometer is used, and it is mounted on the test bearing housing (10). The motor is operated for 3 different speeds of 600 rpm, 700 rpm and 800 rpm. The sampling scale is considered as 5 Hz.

50 samples of each condition are collected with 450 data points in the time domain as well as in the frequency domain. The different defect conditions are listed in Table 1. The vibration spectrums are acquired in 21 combinations of above-mentioned conditions.

Table 1. Different bearing fault conditions

Sr. No.	Defect	Operating speed (rpm)	Size of the defect (mm)
1	Healthy Bearing (HB1)	600	NA
2	Healthy Bearing (HB2)	700	NA
3	Healthy Bearing (HB2)	800	NA
4	Inner Race Defect (IR1A)	600	0.25
5	Inner Race Defect (IR2A)	700	0.25
6	Inner Race Defect (IR3A)	800	0.25
7	Inner Race Defect (IR1B)	600	0.5
8	Inner Race Defect (IR2B)	700	0.5
9	Inner Race Defect (IR3B)	800	0.5
10	Outer Race Defect (OR1A)	600	0.25
11	Outer Race Defect (OR2A)	700	0.25
12	Outer Race Defect (OR3A)	800	0.25
13	Outer Race Defect (OR1B)	600	0.5
14	Outer Race Defect (OR2B)	700	0.5
15	Outer Race Defect (OR3B)	800	0.5
16	Inner and Outer Race Defect (IOR1A)	600	0.25
17	Inner and Outer Race Defect (IOR2A)	700	0.25
18	Inner and Outer Race Defect (IOR3A)	800	0.25
19	Inner and Outer Race Defect (IOR1B)	600	0.5
20	Inner and Outer Race Defect (IOR2B)	700	0.5
21	Inner and Outer Race Defect (IOR3B)	800	0.5

The theoretical formulae to calculate the fault frequency for rolling element bearings considering that the rotation of the innermost race and exterior race is fixed are as follows:

$$F_{\mathrm{BPFI}} = \left[\left(\frac{n}{2}\right)\left(\frac{N}{60}\right)\left(1 + \frac{d}{D}\cos\alpha\right)\right], \tag{1}$$

$$F_{\mathrm{BPFO}} = \left[\left(\frac{n}{2}\right)\left(\frac{N}{60}\right)\left(1 - \frac{d}{D}\cos\alpha\right)\right]. \tag{2}$$

where, N – speed of shaft rotation in rpm, n – number of Rolling members (balls), D – bearing pitch diameter, d – diameter of the rolling member, α – bearing contact angle, F_{BPFI} – Ball Pass Frequency at the Inner race, F_{BPFO} – Ball Pass Frequency of an Outer race.

Table 2 shows the dimensions of the bearing used for the theoretical calculation of fundamental fault frequencies. The F_{BPFO} and F_{BPFI}, calculated for 3 operating speeds such as 600 rpm, 700 rpm and 800 rpm by solving Equation (1) and Equation (2) are listed in Table 3.

Table 2. Bearing specifications

Parameter	Value
Number of rolling members (n)	7
Bearing Pitch diameter (D)	43.38 mm
Ball diameter (d)	11.27 mm
Bearing contact angle (α)	0°

Table 3. Defect frequencies for different operating frequencies

Operating frequency (Hz)	F_{BPFI} (Hz)	F_{BPFO} (Hz)
10	44.09	25.90
11.66	51.44	30.22
13.33	58.79	34.54

Fig. 4 depicts the frequency spectrum obtained from data acquisition system for healthy and a faulty bearing with a 0.25 mm defect at inner race operating at 600 rpm. The defect is characterized by BPFI 46.37 Hz along with two sidebands, whereas the healthy bearing shows maximum amplitude at 1X of the operating

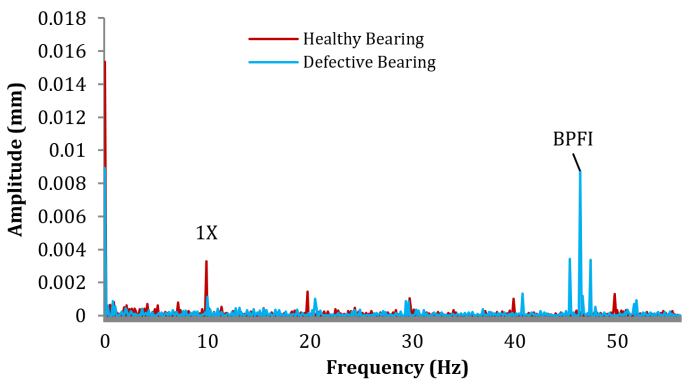

Fig. 4. Comparison of frequency domain plot for healthy and bearing with inner ring raceway fault of 0.5 mm for an operating speed of 600 rpm

frequency. The experimental BPFI is very close to the calculated BPFI. Some discrepancy appears because the speed is not constant during the experimental investigation. There is a distinct increment in the vibration amplitude as the severity of fault grows but the defect frequency and it's nature remains the same which can be clearly observed in Fig. 5.

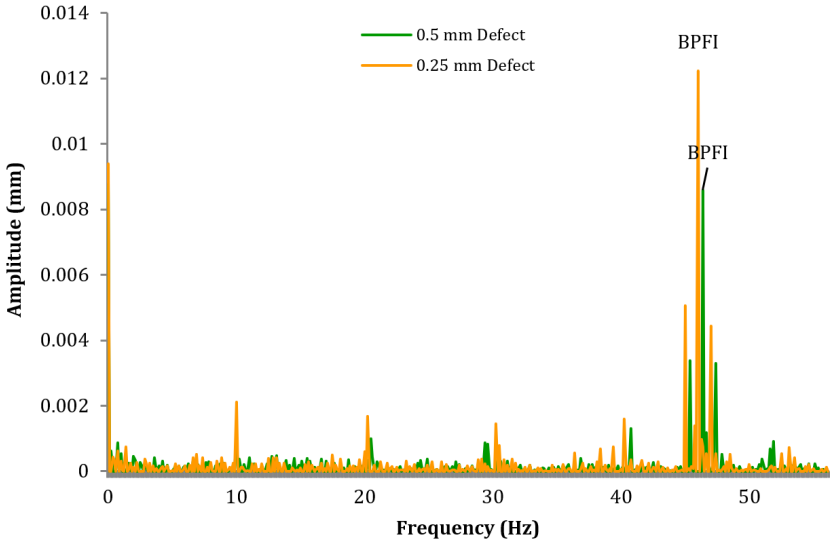

Fig. 5. Comparison of frequency spectrum of defective bearing having a fault severity of 0.25 mm and 0.5 at inner ring raceway for an operating speed of 600 rpm

3. Finite element analysis of bearing defects

For analyzing bearing's vibration behavior pattern in its running condition, it is important to investigate its dynamic response at various fault conditions and operating speeds. Experimental analysis is not always suitable every time because of its limitations. To generate the fault data experimentally, one has to wait till the bearing fails or has to create a defect in a healthy bearing. Finite element analysis is a proven simulation tool to study the dynamic vibration characteristics of machine elements. The method to generate vibration data for different fault conditions (mentioned in Table 1) using ANSYS software is presented in this section. The steps used for vibration signature detection of rotor bearing system are the following: preprocessing, processing and post processing. Preprocessing includes preparation of a solid model.

CAD model of rotor bearings assembly was modelled in Autodesk Inventor 2022 considering the same dimensions as of experimental test rig components shown in Fig. 6. In short a digital twin of the machine has been prepared.

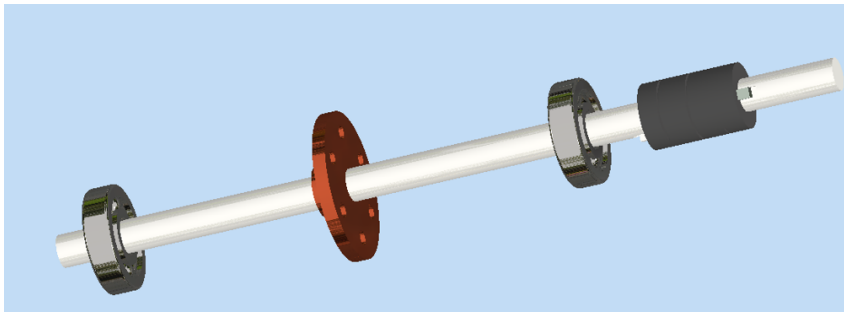

Fig. 6. CAD model of the rotor bearings arrangement

Different models are considered for the analysis. The aim is to check whether the unique vibration characteristics is dependent on the defect size, and speed of the rotor, or not. Fig. 7 shows a bearing having 0.25 mm fault at inner raceway. All the 21 defect conditions were considered for simulation as depicted in Table 1 and accordingly 21 bearing models were prepared. To import the CAD models in FEA software for simulation, they were first exported to the .iges file format. Table 4 gives the material properties of mild steel and aluminum. The driven shaft, driver shaft are made up of mild steel. Coupling is made up of aluminum because it is light in weight, and assembled with a rubber spider.

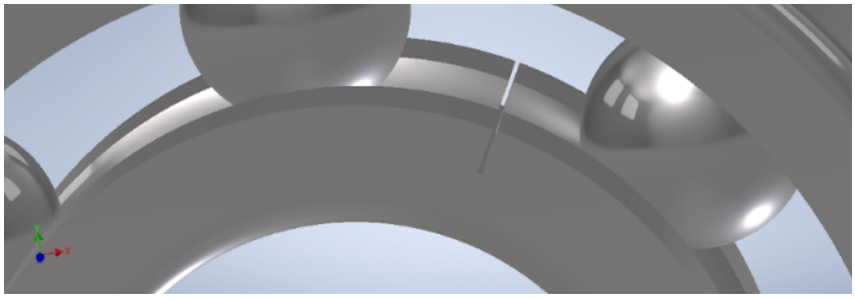

Fig. 7. 0.25 mm fault at innermost raceway

Table 4. Material properties for shaft bearing system

Material	Aluminum	Mild steel	Rubber
Modulus of Elasticity (MPa)	0.675×10^5	2×10^5	30
Poison's ratio	0.334	0.3	0.49
Density (kg/mm^3)	2700×10^{-9}	7850×10^{-9}	1140×10^{-9}

Rubber is assumed to behave linearly. Therefore it can be described using modulus of elasticity and the Poisson's ratio at an initial stage. Actually, it behaves in a nonlinear manner. To take into account this non linearity, Mooney Rivlin

constants were given as an input to define it as a hyperelastic material. These constants are indirectly linked to modulus of rigidity of rubber. The input of Mooney Rivlin constants given for the simulation study are listed in Table 5.

Table 5. Mooney Rivlin constants for rubber [9]

C_1	C_2	C_3	C_4	C_5	C_6	C_7	C_8	C_9
58.66	0.774	54.26	–117.49	52.77	3.58	–23.067	33.69	–12.486

Fig. 8 depicts the meshed view of the CAD model. The element type used for bearing representation between the shaft and the inner ring is COMBIN40 because of its cross-coupling ability. It has a spring and damper arrangement with two nodal points. Each nodal point is associated with a single degree of freedom. The stiffness input assumed for the element is 1.5×10^4 N/mm. The rotational motion is constrained along Y and Z axis (ROTY, ROTZ). The shaft and inner race are allowed to rotate about X-axis. The linear motion is restricted along all three axes, ie., UX, UY and UZ.

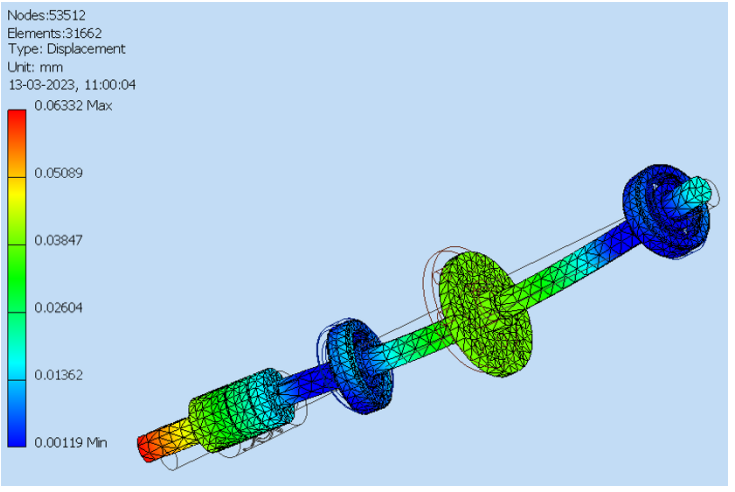

Fig. 8. Meshed model of shaft bearing system

For all the models the element type used is SOLID 186. To generate contact between balls and races TARGET 170 and CONTA 174 elements were used. At the inner race UZ, ROTX and ROTY constrains were given. The radial forces acting on the bearing were calculated manually (Fx = 20.46 N, Fy = 4.468 N). There is no force in axial direction. The maximum frequency is considered to be 60 Hz with a sub step of 5 Hz. The analysis is carried out for 3 different operating speeds viz, 600 rpm, 700 rpm and 800 rpm. The time domain and frequency domain graphs were obtained from the time history postprocessor.

As the mesh size varies the accuracy of the results is affected. The grid independency test confirms the obtained solution's invariance s by means of smaller elements are added to the mesh to refine it. It gives the optimum mesh size for a good accuracy. A mesh independence study was conducted to guarantee independent results from the mesh element size changing from coarse to finer mesh sizes. As the convergence has occurred at a mesh size 31662 with 53512 nodes, the same size was chosen for the analysis. Fig. 8 shows the meshed model depicting displacement contours.

The conclusions drawn from the simulation study are:

- The healthy condition is characterized by 1X of the shaft speed.
- Vibration spectrum shows dominant peak of significant amplitude at BPFI, if the fault is present at inner race.
- Vibration spectrum shows a peak of dominant amplitude at BPFO, if the fault is present at outer race.
- This characterization remains the same irrespective of the speed.
- Analytical and simulated values are in good agreement with each other.

4. Simulation-driven methodology for bearing fault identification

In this work, the proposed simulation-driven approach uses simulated time domain data of healthy and defective bearings at various operating speeds and different fault severities obtained from Finite Element Analysis (FEA) in ANSYS.

Fig. 9 shows the flowchart of the approach derived using simulation data to detect faults in a bearing. The simulation data does not contain any noise signal but the experimental data does. Therefore, 10% Additive White Gaussian Noise (AWGN) is included in the time domain data to obtain a resemblance with the experimental vibration data. The data in time vs amplitude format was represented into Time frequency domain data by applying Wavelet Packet Transform (WPT). Once the transformation is done, a feature extraction procedure is carried out to choose the most influencing features for classifying the data in the 21 categories.

The datasets are then prepared for each category and given as input for training to Machine Learning algorithm, i.e., Multiclass Support Vector Machine (MSVM). To verify the accuracy of the proposed system, the data acquired from the fault simulating test rig was used. Before feeding it to ML algorithm, the data was transformed into time frequency domain and then the features were calculated. As the experimental data already contains noise signals, there is no need to add AWGN to the experimental data. The working principles of signal processing and MSVM are described below.

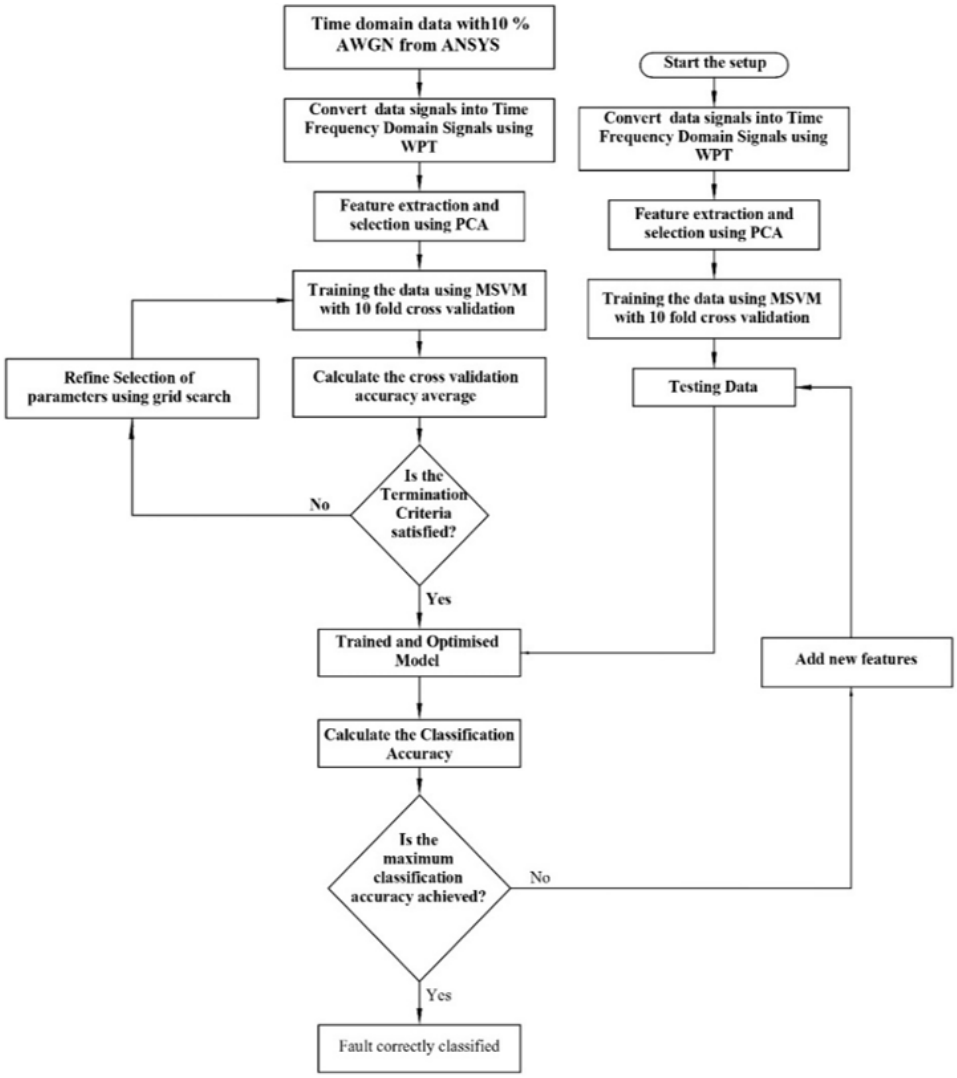

Fig. 9. Flowchart of simulation-driven methodology for bearing fault detection

4.1. Wavelet Packet Transform (WPT)

Wavelet Packet Transform (WPT) and Discrete Wavelet Transform (DWT) have nearly identical format. Both utilize the Multi-Scale Approximation (MSA) Architecture. The primary distinction between DWT and WPT is that, although DWT will have varied frequency bandwidths, WPT has the exact identical frequency bandwidths in every resolution. The amount of information included in the original signals is never increased or decreased during the decomposition pro-

cess. The signal can therefore provide a superior time-frequency analysis if it has a large number of medium and high frequency components. Because the identical frequency bandwidths may deliver adequate resolution independent of highest and lowest frequencies, this transform is well suited for signal processing, particularly nonstationary signals. To correlate it with the Fourier Transform, the basic functions in sine and cosine format are global in amplitude vs time plot but in WPT they are treated as localized functions [10]. A function $W^n_{i,j}(t)$ for WPT can be defined as,

$$W^n_{i,j}(t) = 2^{\frac{i}{2}}, \qquad W^n\left(2^i t - j\right), \tag{3}$$

where i, j are the integers reflecting the wavelet's scale values, and translation values respectively. n is an operation modulation parameter. The first and the second wavelet functions, at $n = 0$ and 1, respectively, are where the scaling expression and mother wavelet expressions are formulated, and they can be written as,

$$W^0_{0,0}(t) = \phi(t), \qquad W^1_{0,0}(t) = \psi(t); \tag{4}$$

at $n = 2, 3, \ldots$ the recursive formulas are expressed as follows:

$$\begin{aligned} W^{2n}_{0,0}(t) &= \sqrt{2}\sum_j h(j) W^n_{1,j}(2t - j), \\ W^{2n+1}_{0,0}(t) &= \sqrt{2}\sum_j g(j) W^n_{1,j}(2t - j) \end{aligned} \tag{5}$$

where $h(j)$ and $g(j)$ are the quadrature mirror filters (QMF) related to the mother wavelet expression and the preset scaling expression. Using the predefined filters represented in a hierarchical multi-resolution, the original signal is decomposed in a recursive manner. The complexity of signal decomposition is largely dependent on the scale and mother wavelet selection. Therefore, an investigation on choosing the best wavelets for the bearing defect classification is made in this study. Table 6 lists the specifics of the four wavelet families that are taken into consideration. The original signal is kept at level 0, and all layers of the decomposition layer are assigned a specific level number.

Table 6. Wavelet families for WPT

Sr. No.	Wavelet family	Wavelet order
i	Haar	db 1
ii	Daubechies	db 2, db 3, db 4, db 5, db 6, db 7, db 8, db 9, db 10
iii	Coiflets	coif 1, coif 2, coif 3, coif 4, coif 5
iv	Biorthogonal	bior 1.1, bior 1.5, bior 2.2, bior 2.6, bior 2.8, bior 3.3, bior 3.7

If i is a level of decomposition, then the number of bases for level i can be calculated as 2^i. Considering the operating speed range, BPFI and BPFO,

the Nyquist frequency is selected as 120 Hz. A two-level signal decomposition is shown in Fig. 10. The clarity of the time frequency data enhances while the signal energy is spread in a uniform manner as the level of breakdown rises [11]. Therefore, in this application, the adequate number of level of decomposition is selected as 2.

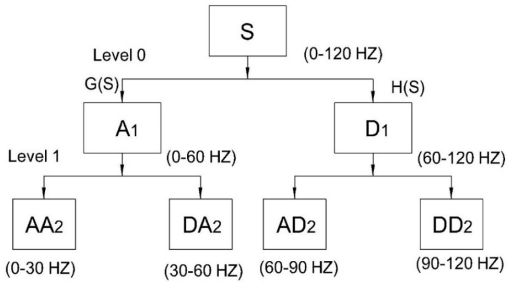

Fig. 10. Decomposition levels of WPT

4.2. Feature extraction and selection using Principal Component Analysis (PCA)

Numerous features including statistical features were proposed by researchers in the literature for detecting faults. The dominating features are calculated from the captured vibration data. In this paper, using WPT a raw time domain signal is decomposed in 2 levels using Daubechies db7 as a mother wavelet function as db7 gives the highest classification accuracy at all 3 speeds. This can be clearly observed from Fig. 11.

For feature selection, statistical features like mean (μ), root sum of squares (RSS), standard deviation (σ), sum of squares (SS), reciprocal of the standard deviation (σ_R), Crest Factor (CF), entropy (e), Shape Factor (SF), skewness (γ), Root Mean Square (RMS), kurtosis (k) are utilized [14]. For selecting the optimal characteristics, several researchers have used various approaches, including Principal Component Analysis (PCA), Random Forest (RF), Factor Analysis (FA), Decision Tree (DT), and Independent Component Analysis (ICA) [15].

PCA analyses the raw data to determine the most significant basis for representation. Here, four bases are taken into consideration (AA2, AD2, DA2 and DD2). The fundamental presumption of PCA consists in the assumption that the significant data fluctuations are characterized by a meaningful mobility [11].

Therefore, the sequence of principal components can be selected based on the sequence in which covariances are placed in a decreasing manner. A principal component is retained, if more than 70% of the data covariance exists, others are removed. Each bases vector is considered as a component to perform PCA from both the levels of WPT decomposed signal. The features are then extracted from the retained principal components. In order to obtain the highest fault prediction

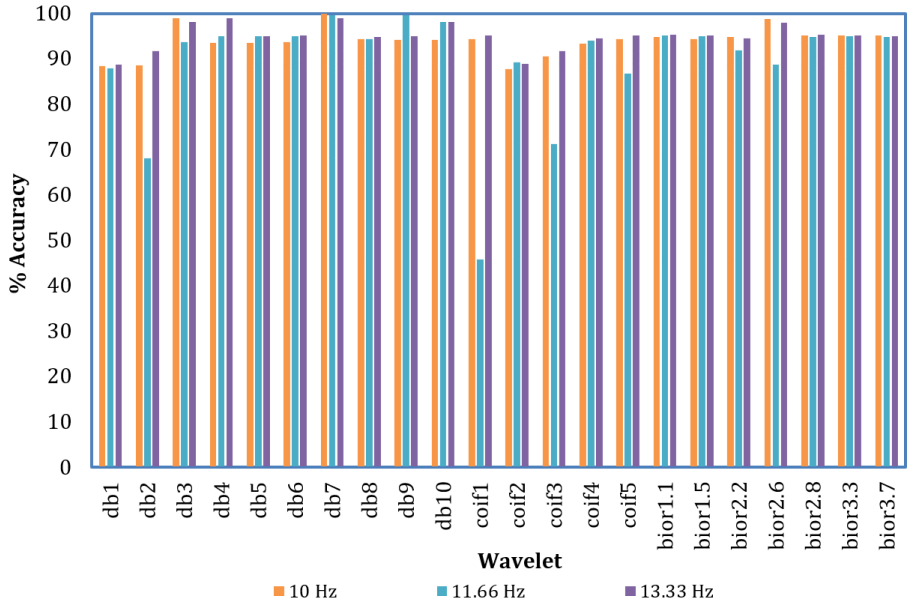

Fig. 11. Fault prediction accuracy of selected wavelets

accuracy, the best or most influencing statistical features were selected with the help of the Wrapper model. Actually, PCA is used for the reduction of dimensionality. But in the proposed work, PCA is used to select bases of WPT.

4.3. Multiclass Support Vector Machine (MSVM)

Generally, Machine Learning Algorithms can be categorized as Supervised Machine learning algorithms and Unsupervised Machine learning algorithms. MSVMs fall under the Supervised Machine learning category and can be used to create new expert and intelligent systems. Vapnik [12] introduced this method for classification as well as for regression analysis for a dataset having limited size of samples. This linear binary classifier follows a non-probabilistic approach.

Fig. 12 depicts how the SVM classifier classifies the data using a boundary plane known as the hyperplane. This boundary is to be maximized for better classification between the two classes. The data points responsible for constructing the margin are known as support vectors. The quadratic function is minimized under linear inequality constraints. Let a training set of N number of sample points be $L = \{(xi, yi)\}$; $(i = 1, 2, \ldots, N)$. Now, the aim is to decide the optimum boundary which will separate the data with the least error. In Fig. 12 triangles and squares represent two classes (one is a negative and another is a positive class) and are identified by the labels $wx + b = -1$ and $wx + b = +1$, respectively.

For non-distinguishable data, slack variables ξ_i are regarded as having a zero or positive value. The following optimization problem can be solved to determine the

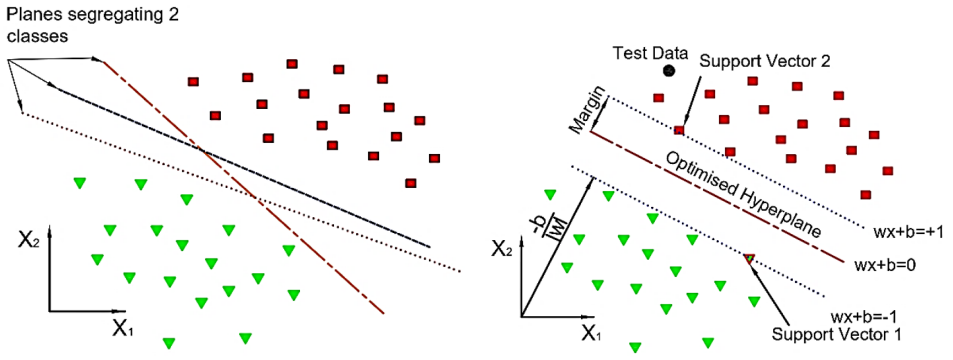

Fig. 12. (a) Possible orientations of hyperplanes in SVM, (b) optimized hyperplane

classifying plane $f(x) = 0$ that divides the input data [13]. In a feature space, positive and negative classes are separated using a linear boundary plane bounded with support vectors. To determine the orientation and location of the boundary plane, the margin is maximized by considering the space between the data classifying plane and the point nearest to the plane called as the support vector.

Once the orientation and location of the separating plane is fixed, another new point can be tested for segregation based on its location with respect to the separating plane. If, $L = \{(xi, yi)\}$; is the input data and $wx + b$ is ± 1 based on the group it is associated with, then the SVM optimization problem can be formulated as,

$$\begin{aligned} &\text{Minimize } \frac{1}{2}\left\|W^2\right\| + C\sum_{i=1}^{N}\xi_i \text{ subject to} \\ &\begin{cases} y_i\left(W^T\,\phi(x_i) + b\right) \geqslant 1 - \xi_i \\ \xi_i \geqslant 0, \quad i = 1, 2, \ldots, N \end{cases} \end{aligned} \tag{6}$$

Here, the weights vector is termed as w, b is considered as bias, and the equilibrium between the complexity of the algorithm and the training error is initiated by C. ξ_i is used to accommodate wrong classification. As the algorithm classifies the data in a binary format, it is necessary to use one-against-one methodology to segregate the multi-class data into a number of binary sets in order to accomplish a multi-class data classification. A multifaced RBF Gaussian kernel is selected in the presented work because of its good data prediction ability. The testing data is matched with all the binary sets of classifiers and subsequently, the votes are noted for each comparison. The data is categorized into a class having a majority of votes.

The classification accuracy thus can be calculated as follows:

$$C_a = \frac{\text{No. of Correct predictions}}{\text{Total number of datasets used for testing}} \times 100. \tag{7}$$

To achieve the desired classification performance, the combination of kernel and SVM parameters have to be chosen properly. In this research, a grid search method is applied with cross validation. First of all, the training data obtained from simulation is arbitrarily divided into h subgroups. Out of k subgroups, $k-1$ are given as an input for the training purpose. The leftover data set is reserved for testing. This procedure is continued for all subgroups of training data and the one remaining as a testing data, to obtain the most precise Support Vectors. After finalizing the parameters, the hyperplane is created and the data obtained from experimentation is used to check the performance. A 10-fold cross-validation procedure is employed in the current system. For choosing the most influencing features for fault identification, the wrapper model is employed. The fault prediction accuracies using WPT-PCA-MSVM can be observed from Fig. 13. The accuracy of statistical features, i.e., RSS and mean, is observed to be greater than 99.4%. Thus, this union of features is fixed for classifying the data. This simulation-driven approach is named the WPT-PCA-MSVM.

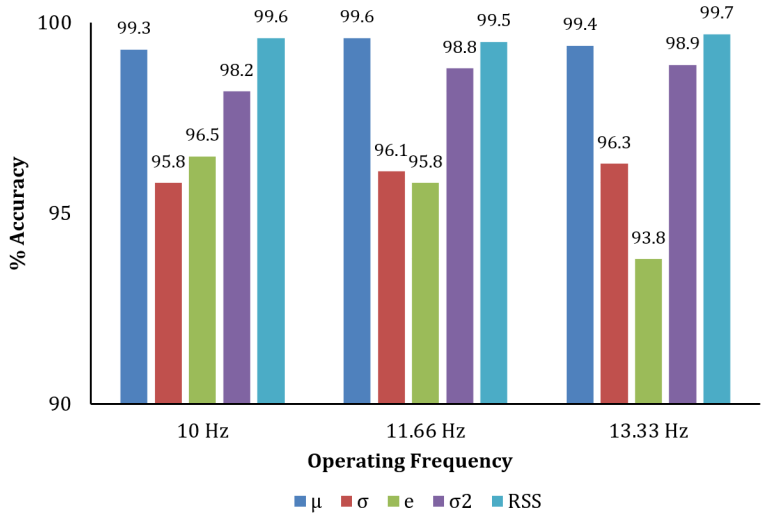

Fig. 13. Accuracy of fault prediction from extracted features using PCA

5. Results and discussion

This research work follows a simulation-driven approach for the identification of bearing defects with due consideration of the severity of the defect using machine learning. The analytical unique fault identification frequencies such as BPFO and BPFI are evaluated using Eq. (1) and Eq. (2) as tabulated in Table 3. The experimental fault frequency data is collected using FFT analyzer as discussed in Section 2. The simulated fault frequencies are obtained using ANSYS, which is briefly described in Section 3. Fig. 14 to Fig. 17 depicts the comparison of

analytical, experimental and simulation fault frequencies for all the bearing defect conditions mentioned in Table 1. It can be observed that the analytical BPFO and BPFI values are not affected by the severity of the fault. Simulation results fit well analytical and experimental results. The approximate error between analytical and simulated frequencies is 3.5% and that between analytical and experimental one is 7.8%.

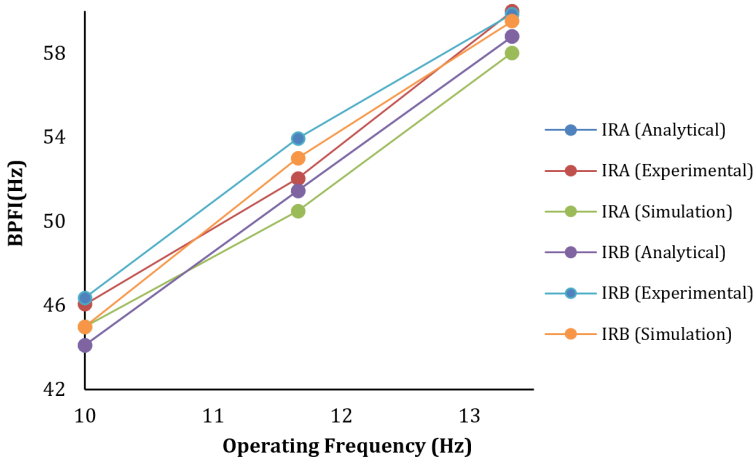

Fig. 14. Comparison of analytical, experimental and simulation BPFI for defect at inner race

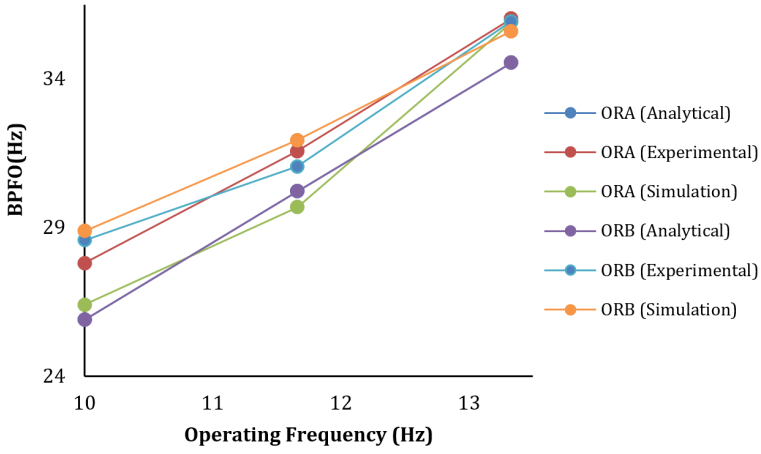

Fig. 15. Comparison of analytical, experimental and simulation BPFO for defect at outer race

In experimental results, a small variation in fault frequency is seen as compared to analytical fault frequencies. It occurs because of speed fluctuation, whereas the variation is also observed in simulation results which is due to the addition of noise signals.

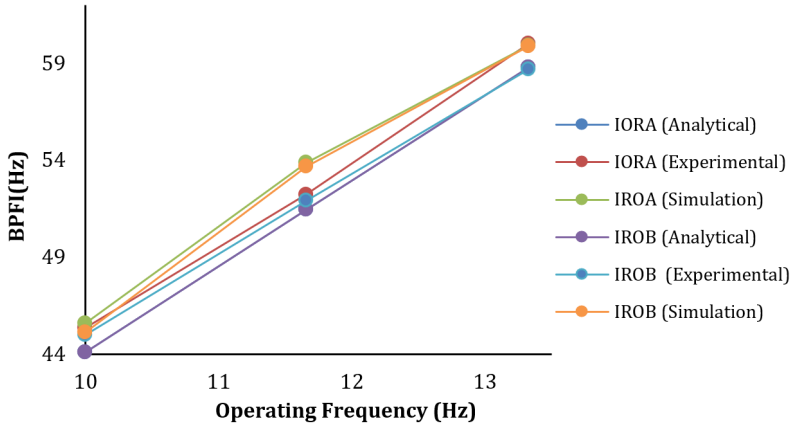

Fig. 16. Comparison of analytical, experimental and simulation BPFI for defect at inner and outer race

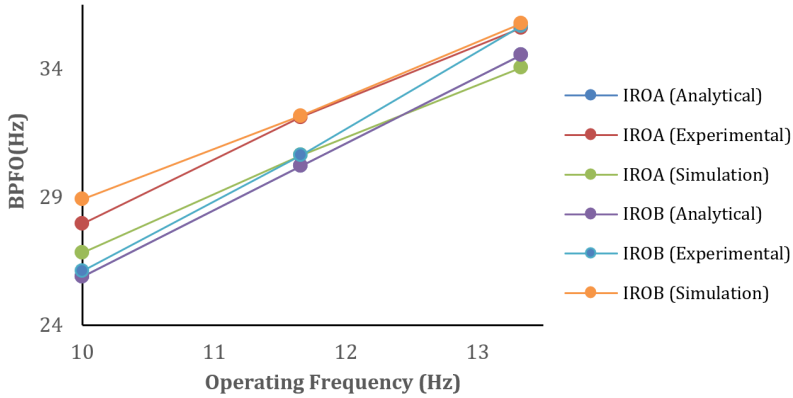

Fig. 17. Comparison of analytical, experimental and simulation BPFO for defect at inner and outer race

Beside of the known operating frequencies, the experimental data was collected for some unknown operating frequencies to test the accuracy of the developed system for these unknown frequencies, as illustrated in Fig. 19, Fig. 21 and Fig. 23. In the data driven approach, experimental vibration data is used for training as well as for testing purpose. This simulation-driven procedure uses the simulation data for training and experimental data for testing purpose. Fig. 18 to Fig. 23 shows the comparison of accuracies obtained from the data-driven approach and simulation-driven approach for inner raceway fault, fault in outer raceway and for the combined defect at inner and outer raceways respectively.

Though the machine learning algorithm was trained for 3 different speeds viz, 600 rpm (10 Hz), 700 rpm (11.67 Hz) and 800 rpm (13.33 Hz), the algorithm was capable to detect bearing faults at any unknown operating speed too. The accuracy

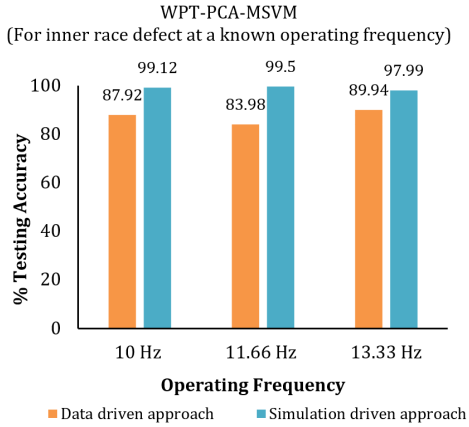

Fig. 18. Testing accuracies of data-driven and simulation-driven approach for defect at inner race at known operating frequency

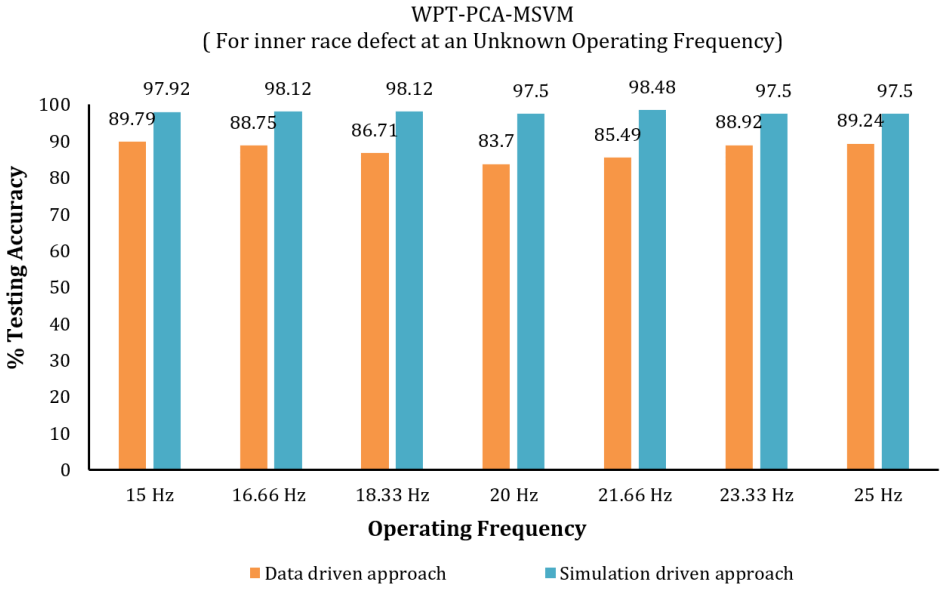

Fig. 19. Testing accuracies of data-driven and simulation-driven approach for defect at inner race for an unknown operating frequency

of known operating speed data is around 98.82% for all the defects under consideration using simulation-driven approach. The algorithm was tested for different unknown operating speeds for which the algorithm was not trained. For an unknown operating speed test data, the accuracy of the proposed model is observed as 98.03%. It can be seen in Fig. 19 to Fig. 23 that the simulation-driven approach gives highest testing accuracy for all operating speeds. Also, the model was tested

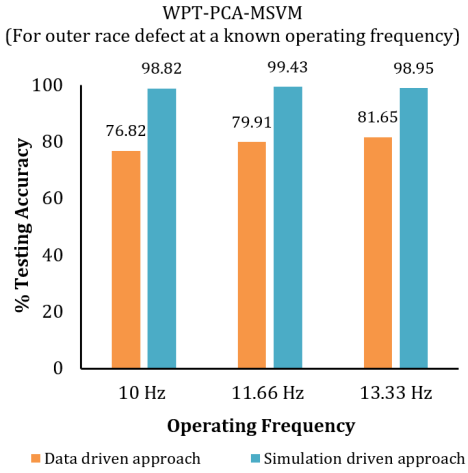

Fig. 20. Testing accuracies of data-driven and simulation-driven approach for defect at outer race for a known operating frequency

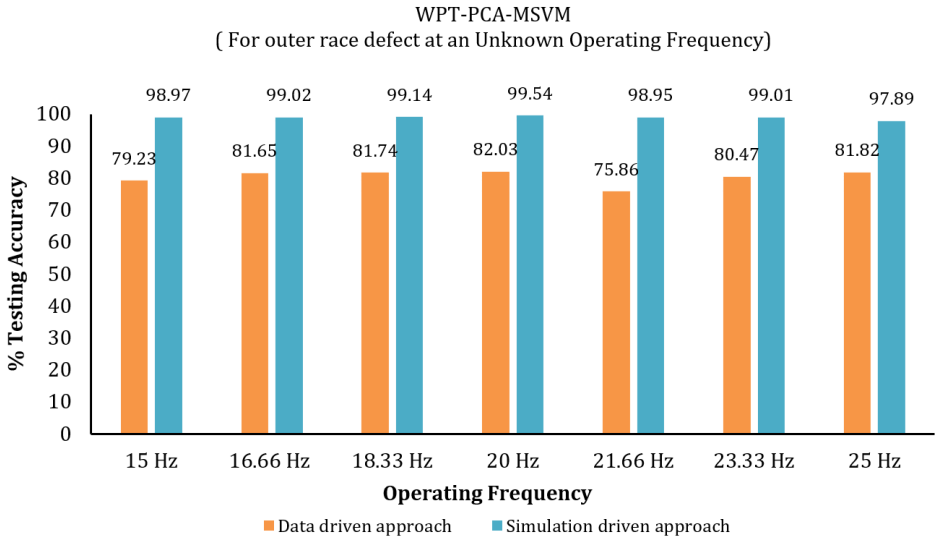

Fig. 21. Testing accuracies of data-driven and simulation-driven approach for defect at outer race for an unknown operating frequency

for the available datasets from mfpt.org [18], and it was able to detect the defect in the bearing successfully. Therefore, the model can be generalized for all ball bearings. A comparison between the proposed model and the models available in the literature is presented in Table 7. The parameters used for the comparison are faults considered, type of data, considered severity of the fault, feature selection technique, features selected, machine learning technique used, approach and accuracy. It can be proved that simulation-driven approach gives a better accuracy

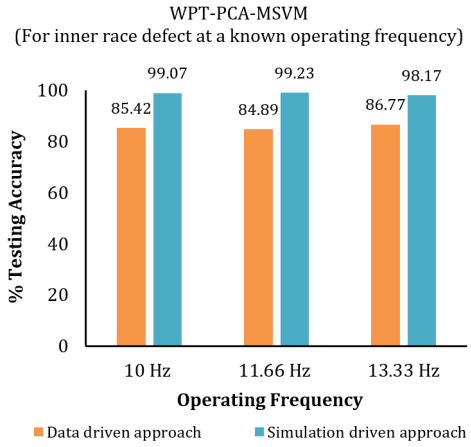

Fig. 22. Testing accuracies of data-driven and simulation-driven approach for defect at inner and outer race for a known operating frequency

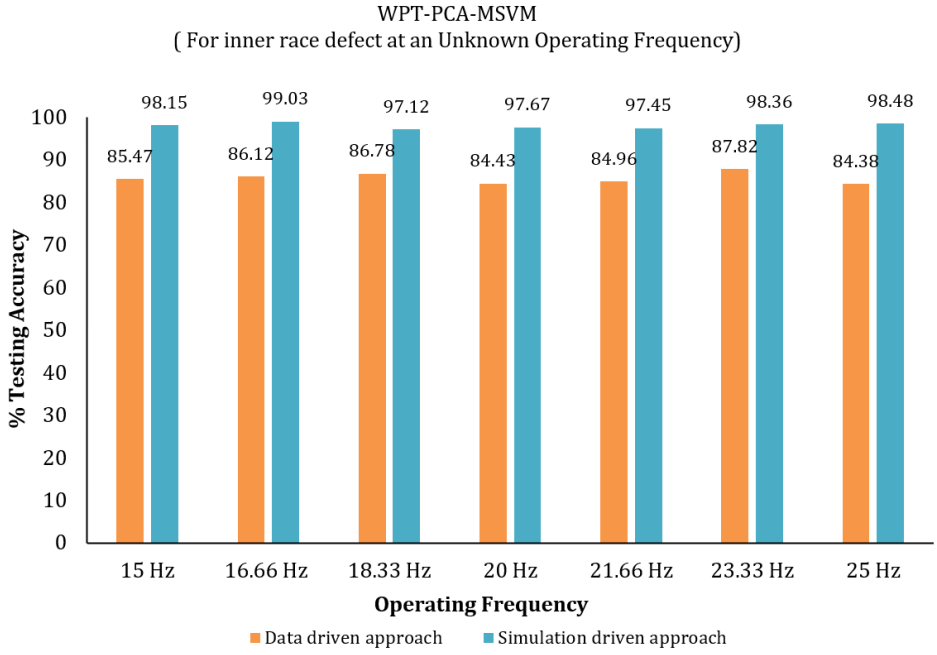

Fig. 23. Testing accuracies of data-driven and simulation-driven approach for defect at outer race for an unknown operating frequency

in the absence of historic data. In this technique, by developing a digital twin of any machine, the most likely faults and their vibration behavior can be easily predicted.

Table 7. Comparison between proposed model and the models available in the literature

Parameters	References				
	Minhas et al. (2019) [17]	Patil, S., Phalle, V. (2018) [16]	Ratnam et al. (2018) [5]	Kankar et al. (2011) [7]	Pallavi Khaire, V.M. Phalle (Present Work)
Faults Considered	Single	Combination	Single	Combination	Single and Combination
Type of data representation	Time Domain	Time Domain	Time Domain	Time Domain	Time-Frequency Domain
Severity of Fault	Yes	No	Yes	No	Yes
Feature Selection Technique	Ensemble Empirical Mode Decomposition	Decision Tree, Randomized Lasso	NA (Features were randomly chosen)	Maximum Energy to Shannon Entropy ratio for Meyer and Complex Morlet Wavelet	Principal Component Analysis
Machine Learning classification Technique	Refined Composite Multi-Scale Fuzzy Entropy	Random Forest, Decision Tree, Support Vector Machine, Extra Tree Classifier, Gradient Boosting Classifier	Support Vector Machine, Artificial Neural Networks	Support Vector Machine, Artificial Neural Networks, self-organizing maps	Multiclass Support Vector Machine
Approach	Data Driven	Data Driven	Data Driven	Data Driven	Simulation Driven
Accuracy	99%	98.12%	93.43%	98.67%	98.82%

6. Conclusions

The fault prediction accuracy of WPT-PCA-MSVM in the proposed model is considerably good because of SVM's excellent generalization and classification ability, as compared to other machine learning approaches published by researchers. MSVM can be used as an efficient tool for identifying bearing defects, which allows for avoiding catastrophic failures likely to occur in future. This supervised machine learning technique gives the best classification accuracy of 98.82% using simulation-driven approach in the proposed model.

The PCA-based approaches of bases selection are fairly simple to understand and apply in real-world settings [11]. The healthy condition of the bearing is observed by determining the maximum amplitude at 1X of the operating frequency in the frequency domain plot. Inner race and outer race defects are mainly characterized by BPFI and BPFO, respectively. These unique features remain unchanged for different speeds and severity of the defect. But for the same operating speed, as the severity increases, the amplitude of vibration at BPFO and BPFI increases. This novel simulation model works efficiently to identify a single fault and combination

of faults in a rolling element bearing. The expertise of vibration analysis is not required to detect faults using this machine learning model. Any unskilled person can feed the data to the algorithm and detect the fault and take a corrective action. As the model follows simulation-driven approach, it does not require any historic data to train the algorithm. The algorithm also works if for a particular machine historic data is not available. A digital twin for different machinery faults can be simulated, and the training data can be generated as and when it is required. The number of data sets can be simulated for healthy, faulty conditions and used for training as and when required using a digital twin of the machine. The drawback of the proposed system is, that it requires more computation time to generate simulation data. The computation time varies according to the complexity of the model. The accuracy of the trained model depends upon the amount of AWGN added. Also, appropriate instrumentation is required to acquire the vibration data. As the machine learning model learns itself and uses extracted statistical features, the model can be used to detect the defect in any ball bearing. The machine learning code may be converted into a web application which will facilitate identifying the damaged bearing from any remote location. Thus it can be concluded that Simulation-driven condition monitoring using machine learning models is an efficient and smart tool for rolling element-bearing fault detection in the Industry 4.0.

References

[1] Z. Taha and N.T. Dung. Rolling element bearing fault detection with a single point defect on the outer raceway using finite element analysis. *The 11th Asia Pacific Industrial Engineering and Management Systems Conference and the 14th Asia Pacific Regional Meeting of International Foundation for Production Research*, Melaka, Malaysia, 7-10 Dec. 2010.

[2] P. Jayaswal, S.N. Verma, and A.K. Wadhwani. Development of EBP-Artificial neural network expert system for rolling element bearing fault diagnosis. *Journal of Vibration and Control*, 17(8):1131–1148, 2011. doi: 10.1177/1077546310361858.

[3] V.V. Rao and Ch. Ratnam. A comparative experimental study on identification of defect severity in rolling element bearings using acoustic emission and vibration analysis. *Tribology in Industry*, 37(2):176–185, 2015.

[4] S. Shah and A. Guha. Bearing health monitoring. *Tribology in Industry*, 38(3):297–307, 2016.

[5] C. Ratnam, N.M. Jasmin, V.V. Rao, and K.V. Rao. A comparative experimental study on fault diagnosis of rolling element bearing using acoustic emission and soft computing techniques. *Tribology in Industry*, 40(3):501–513, 2018. doi: 10.24874/ti.2018.40.03.15.

[6] K. Kappaganthu and C. Nataraj. Modelling and analysis of outer race defects in rolling element bearings. *Advances in Vibration Engineering*, 11(4):371–384, 2012.

[7] P.K. Kankar, S.C. Sharma, and S.P. Harsha. Fault diagnosis of ball bearings using continuous wavelet transform. *Applied Soft Computing*, 11(2):2300–2312, 2011. doi: 10.1016/j.asoc.2010.08.011.

[8] A. Sharma, M. Amarnath, and P.K. Kankar. Feature extraction and fault severity classification in ball bearings. *Journal of Vibration and Control*, 22(1):176–192, 2014. doi: 10.1177/1077546314528021.

[9] V. Hariharan and P.S.S. Srinivasan. Vibration analysis of parallel misaligned shaft with ball bearing system. *Sonklanakarin Journal of Science and Technology*, 33(1):61–68, 2011.

[10] J.D. Wu and C.H. Liu. An expert system for fault diagnosis in internal combustion engines using wavelet packet transform and neural network. *Expert Systems with Applications*, 36(3):4278–4286, 2009. doi: 10.1016/j.eswa.2008.03.008.

[11] J.S. Rapur and R.Tiwari. Experimental fault diagnosis for known and unseen operating conditions of centrifugal pumps using MSVM and WPT based analyses. *Measurement*, 147:106809, 2019. doi: 10.1016/j.measurement.2019.07.037.

[12] C. Cortes and V. Vapnik. Support vector network. *Machine Learning*, 20(3):273–297, 1995. doi: 10.1007/BF00994018.

[13] S. Damuluri, K. Islam, P. Ahmadi, and N.S. Qureshi. Analyzing navigational data and predicting student grades using support vector machine. *Emerging Science Journal*, 4(4):243–252, 2020. doi: 10.28991/esj-2020-01227.

[14] R. Tiwari. *Rotor Systems: Analysis and Identification*. CRC Press, 2017. doi: 10.1201/9781315230962.

[15] V.C. Handikherkar and V.M. Phalle. Gear fault detection using machine learning techniques – A simulation-driven approach. *International Journal of Engineering*, 34(1):212–223, 2021. doi: 10.5829/IJE.2021.34.01A.24.

[16] S. Patil and V. Phalle. Fault detection of anti-friction bearing using ensemble machine learning methods. *International Journal of Engineering*, 31(11):1972–1981, 2018.

[17] A.S. Minhas, G. Singh, J. Singh, P.K. Kankarand, and S. Singh. A novel method to classify bearing faults by integrating standard deviation to refined composite multi-scale fuzzy entropy. *Measurement*,154:107441, 2020. doi: 10.1016/j.measurement.2019.107441.

[18] www.mfpt.org.